CDRI ◇

UN
DP

**Global Infrastructure Resilience**
Capturing the Resilience Dividend

**Global Drought impact on Hydropower, Water Use and Fluvial Navigation**

CIMA Foundation, Italy

Position Paper | 2023

cimα
RESEARCH
FOUNDATION

Obser

# GIRI

# Global Infrastructure Risk Model and

# Resilience Index

Contract 2021/219

Drought Risk Computations

# Consortium

Centro Internazionale in Monitoraggio
Ambientale CIMA Research Foundation
Via A. Magliotto, 2, Savona-17100, ITALY
www.cimafoundation.org

UNIVERSITÉ DE GENEVE
24 rue du Général-Dufour, 1211 Genève
www.unige.ch

Norwegian Geotechnical Institute NGI
PO Box 3930 Ullevaal Stadion, N-0806 Oslo
www.ngi.no

INGENIAR CAD/CAE Ltda.
Carrera 19A # 84-14 OF 504, Bogotá
www.ingeniar-risk.com

| Version Number | Description | Authors | Approved by | Date |
|---|---|---|---|---|
| 1.0 | First release | Roberto Rudari Carmelo Camalleri, Tatiana Ghizzoni, Lauro Rossi, Michel Isabellon | Roberto Rudari | 11/04/2023 |

## CONTENTS

# 1    BACKGROUND

The Coalition for Disaster Resilient Infrastructure (CDRI) was launched by the Government of India in September 2019 at the UN Climate Action Summit. The CDRI is a partnership of national governments, UN agencies and programs, multilateral development banks and financing mechanisms, the private sector, and knowledge institutions that aims to promote the resilience of new and existing infrastructure systems to climate and disaster risks, thereby ensuring sustainable development. The CDRI intends to publish a biennial Flagship report on Disaster and Climate Resilient Infrastructure. The report will be CDRI's principal vehicle for engaging and focusing the attention of a global audience of political leaders, policy makers, practitioners, and researchers.

The Flagship report will contribute to the development of the Strategic Priorities of the CDRI around Research and Knowledge Management and Communication and Partnerships. The report is envisaged to be based on five key pillars:

- Pillar 1 Global Infrastructure Risk Model
- Pillar 2 Global Infrastructure Resilience Index
- Pillar 3 Nature Based Solutions
- Pillar 4 Progress Monitoring
- Pillar 5 Financing Infrastructure Resilience

This inception report intends to describe the methodological approach to Pillar 1 and the details of its implementation.

Pillar 1 focuses on the design and implementation of a Global Infrastructure Risk Model. This will entail the update and enhancement of the existing Global Risk Model (GRM) developed for the

United Nations in 2017 for the Global Assessment Report (GAR) along with a sophisticated analysis of the disaster and climate risk to infrastructure systems. It will include developing an infrastructure inventory or proxies, sourcing infrastructure exposure data and vulnerability functions, hazard risk assessment and multi-hazard probabilistic risk modelling. It will contemplate risk to infrastructure in the following sectors (power and energy, transport, and telecommunications) as well as local and social infrastructure and will produce a set of probabilistic financial risk metrics for each country or territory, such as Loss Exceedance Curves (LEC), Average Annual Loss (AAL) and Probable Maximum Loss (PML). Most of the efforts will focus on climate related hazard such as Floods, Droughts and Cyclones in order to capture the climate trends in risk on critical infrastructures connected with RCPs and SSPs that could be unfolding in the near and far future. Earthquakes and tsunami risk will also be computed as they give a critical contribution to risks on infrastructures at global level.

## 2    Hydrological Modelling as a basis for Floods and Droughts Hazard assessment

The hydrological model used is the Continuum model (Silvestro et al. 2013 and 2015). It is a continuous, distributed and physically based hydrological model able to reproduce the spatial-temporal evolution of soil moisture, energy fluxes, surface soil temperature, evapotranspiration and discharge. It was designed to find a balance between a detailed description of the physical processes and a robust and parsimonious parameterisation. The model can consider the presence of dams and other hydraulic structures. The hydrologic model is at the basis of the Hazard assessment both for floods and droughts.

## 3    Drought Hazard modelling

Drought indicators are commonly used tools to describe drought conditions based on key hydro-meteorological variables such as precipitation, temperature, evapotranspiration, soil moisture, streamflow, and groundwater. Due to the variety of dynamics involved in the propagation of drought within the hydrological cycle and the implications for impacted sectors, numerous drought indicators are available in the literature to capture different aspects of the drought phenomenon (WMO and GWP, 2016). Meteorological drought indices aim at capturing the main driver of drought represented by precipitation deficits, agricultural drought indices usually focus on short to medium-term effects of a drought propagating in the hydrological cycle, and hydrological drought indices focus on medium- to long-term effects recorded on slow-responding hydrological variables. Often drought research studies focus on a single drought indicator, selected as the most relevant for the specific application. In this study, we integrated three drought indicators in order to cover all the above mentioned aspects of drought propagation. In particular, we adopted indices based on the meteorological forcing (precipitation) and water balance outputs (soil moisture and streamflow) derived from the Continuum model (see previous sections for further details).

- The standardized precipitation index computed on a 6-month accumulation (SPI-6) aims to capture medium-to-long-term variations in water availability and is commonly used to detect drought occurring at a seasonal scale (WMO, 2012). The indicator is computed by fitting a gamma distribution to the historical records of precipitation (1981-2016 in this study) and transforming the probability value into a normal standardized value.
- The standardized streamflow index (SSI) aims at capturing the dynamics of hydrological droughts commonly associated with medium-term dynamics (Shukla and Wood, 2008). It is computed as a standard z-score (with respect to the baseline 1981-2016) on the monthly average streamflow data.

- Similarly, the soil moisture anomaly (SMA) index is a standardization of the monthly average soil moisture in the root zone (Cammalleri et al., 2016), and it aims to capture the short-term effects of droughts commonly relevant for agricultural studies.

Maps for all three indicators for the two future scenarios, low (SSP1 2.6) and high (SSP5 8.5), are derived for the period 2050-2100 following a similar standardisation procedure but using the baseline statistics computed for the present climate (1981-2016). This procedure allows evaluating the effects of climate change on the drought indicators, by comparing the future condition to a reference that is represented by the present climate.

The maps in Figure 1 show an example of these indicators over Madagascar, highlighting in yellow-to-red shades the areas under deficit, corresponding to the drought conditions, and in blue shades the areas with surplus.



January 2016

SPI-6          SSI          SMA
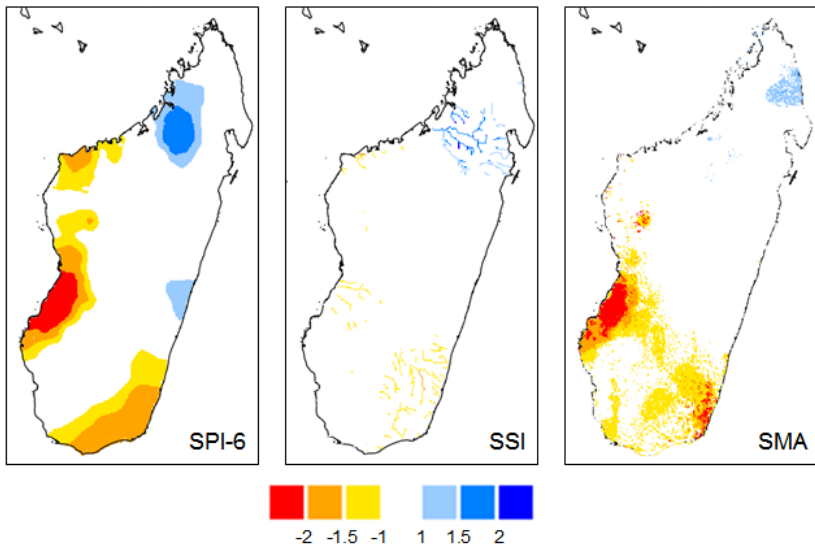
-2  -1.5  -1      1  1.5  2

Figure 1 Examples of SPI-6 (left panel), SSI (central panel), and SMA (right panel) maps for January 2016 over Madagascar.

The combined use of these three indicators allows for accounting for the main temporal scales and processes affecting the propagation of drought events, providing the necessary flexibility to reproduce drought impacts in different sectors worldwide. In fact, it is well-known that drought impacts over different regions may be explained by different indicators, depending on how the drought propagates through the hydrological cycle (Hao and Singh, 2015). The use of multiple indices attempts to overcome this issue, by searching for the optimal combination for each area.

Since the main application, in this study, is the modelling of drought conditions impacting hydropower production, an obvious index choice would be to adopt the SSI index as the main driver of drought conditions impacting the inflow of reservoirs feeding the hydropower energy plants. However, a more holistic approach was preferred in this case in order to capture a larger portion of the variability of hydropower production. The type of analysis will then automatically select the most appropriate combination of indicators in accordance with local morphologies and climates as it will be better explained in the following sections.

To provide a synthetic depiction of the status of drought hazard in the reference present conditions (1980-2016), time series of the three standardised indices were processed to detect continuous periods of drought conditions (also known as events),  following the theory of runs (Yevjevich, 1967). Here, a drought event is **defined as a period longer than three months with the indicator below -1**. Events separated by only a single month gap are pooled together and considered as a continuous event (Zelenhasić and Salvai, 1987).

From this analysis, the average duration of a drought event (in months) and the total number of events in the 37-year period (1980-2016) are derived from the run analysis for each indicator, as reported for example in Figure 2 for the SPI-6 for Madagascar. By knowing the average number of events in the period, a frequency in terms of return period can be defined for each indicator as shown in Figure 3.
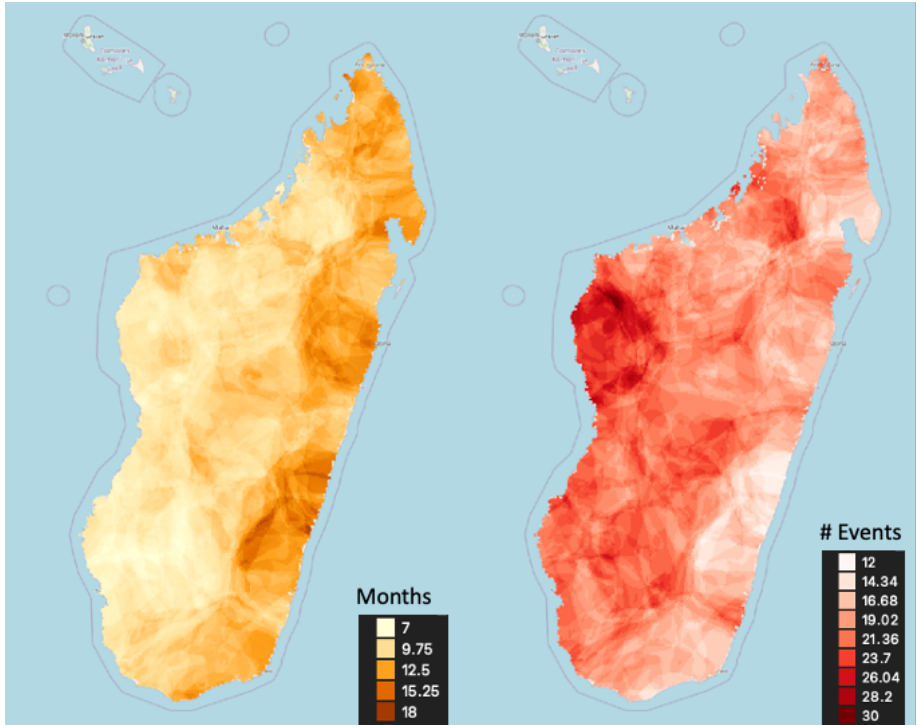
Figure 2. Average duration of drought events in the present climate (left panel) and average number of events in the present climate in the reference period 1981-2016 (right panel) as defined by using SPI-6 as a reference indicator for the Country of Madagascar.
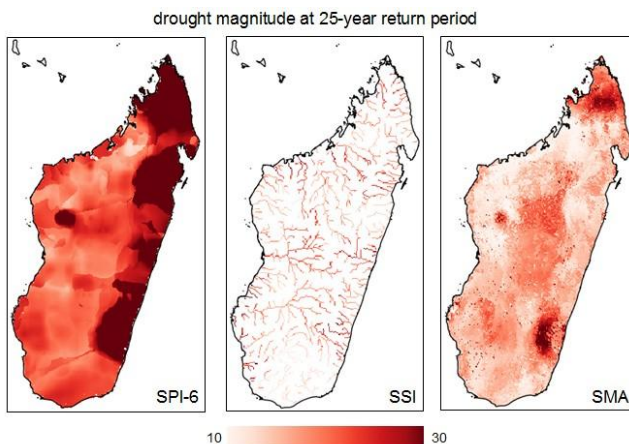
Figure 3. Maps of the drought magnitude at 25-year return period according to SPI-6 (left), SSI (middle) and SMA (right) over Madagascar.

## 3.1 Drought impacts on energy production

Droughts are a natural hazard that develops slowly and can have a broad range of impacts on various sectors of the economy. While some critical infrastructures such as water supply systems can be directly affected by droughts, others such as energy, transportation, or communication systems are rarely impacted directly. However, droughts can have significant indirect economic impacts due to the loss of functionality or efficiency of these critical infrastructures. Hydropower plants require a consistent supply of water to generate electricity, and droughts can significantly reduce the amount of available water, leading to reduced power output or even complete plant shutdown. This can result in power shortages, higher electricity prices, and increased reliance on other energy sources such as fossil fuels. Similarly, droughts can impact transportation systems by reducing the capacity of waterways, leading to reduced shipping traffic and increased

transportation costs. Therefore, while droughts may not have direct impacts on critical infrastructures, they can have significant secondary economic impacts that can affect the overall resilience of the services these infrastructures provide. The following section will focus on the impacts of droughts on hydropower production.

### 3.1.1    Hydropower production as a proxy variable of drought impacts

Drought events can have a significant impact on a country's ability to produce hydropower energy. To understand the relationship between drought indicators and hydropower production at a global scale, a study was conducted on countries where hydropower energy represents a major energy source. The energy production data used in this study were obtained from the BP Statistical Review of World Energy[1] and Ember[2,3]. Countries where hydropower represents more than 75% of the total energy production in the 10-year period from 2011 to 2020, and with a total production (P) greater than 0.5 TWh, were selected for this study and are reported in Table 1.

It is important to note that both long-term trend and inter-annual variability in energy production are not solely controlled by water availability, but they are also influenced by various external factors that dictate energy demand. Therefore, in this study, the fluctuations around the average dynamic were used as a proxy variable to assess the effects of drought events on hydropower production. These fluctuations ($\sigma$) were derived by subtracting the actual recorded data from the average long-term behaviour modelled using a smoothing function (Savitzky–Golay filter). The $\sigma$ values (difference between actual and smoothed values) were then standardised (z) to obtain a

---

[1] https://www.bp.com/en/global/corporate/energy-economics/statistical-review-of-world-energy.html

[2]https://ember-climate.org/data-catalogue/yearly-electricity-data/

[3] https://ember-climate.org/insights/research/european-electricity-review-2022/

standard normally distributed quantity (0 mean and unitary standard deviation).
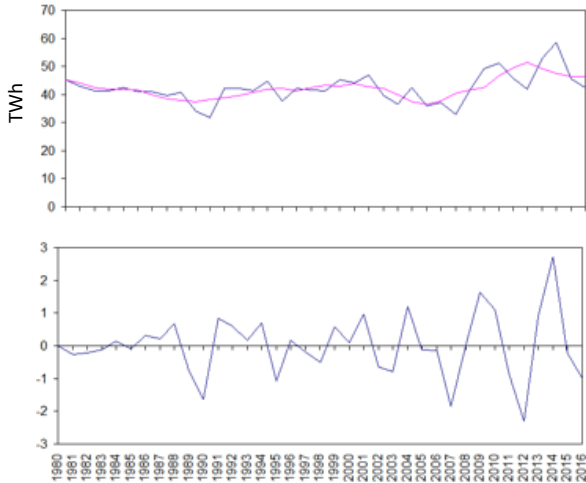


Figure 4 illustrates an example of the procedure adopted to derive standardised variations in hydropower production.

Given the high fraction of energy derived from hydropower in the selected countries, the impact of drought on the energy sector is strongly correlated with the impact on hydropower production. Therefore, it follows that understanding the impact of drought on hydropower production is crucial for ensuring the resilience of the energy sector in countries where hydropower represents a major energy source.

Table 1 Description of the countries selected for the development of hydropower models.

| ISO | Country name | Avg. hydro production (μ) 2011-2020 (TWh) | % total | Year available in 1980-2016 |
|-----|--------------|------------------------------------------|---------|------------------------------|
| AFG | Afghanistan | 0.86 | 83 | 17 |
| ALB | Albania | 5.77 | 99 | 27 |
| BTN | Bhutan | 7.64 | 100 | 17 |
| COD | Congo (Dem. Rep.) | 8.81 | 99 | 17 |
| CRI | Costa Rica | 7.65 | 79 | 17 |
| ETH | Ethiopia | 10.45 | 99 | 17 |
| GEO | Georgia | 8.51 | 79 | 17 |
| KGZ | Kyrgyzstan | 13.33 | 92 | 17 |
| LAO | Lao (People's Dem. Rep.) | 16.82 | 76 | 17 |
| LSO | Lesotho | 0.51 | 100 | 17 |
| MOZ | Mozambique | 15.06 | 87 | 17 |
| MWI | Malawi | 1.72 | 88 | 17 |
| NAM | Namibia | 1.32 | 97 | 17 |

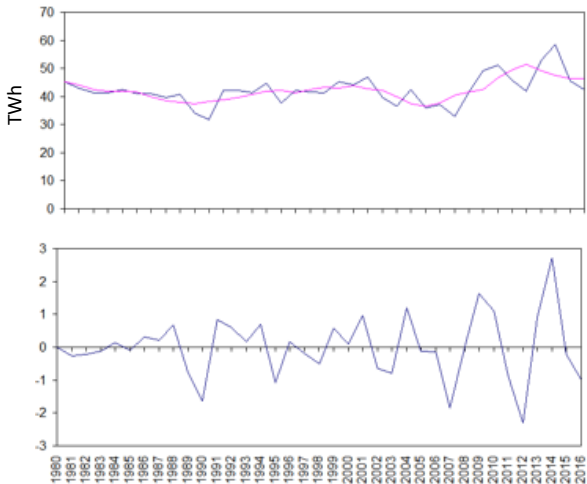| NOR | Norway | 135.33 | 97 | 37 |
|-----|--------|--------|-----|-----|
| NPL | Nepal | 3.84 | 100 | 17 |
| PRK | Korea (Dem. People's Rep.) | 12.59 | 77 | 17 |
| PRY | Paraguay | 56.55 | 100 | 17 |
| TJK | Tajikistan | 17.00 | 96 | 17 |
| UGA | Uganda | 2.94 | 82 | 17 |
| ZMB | Zambia | 12.77 | 92 | 17 |

Figure 4. Example of the procedure to derive the proxy of drought impacts on hydropower production. The upper panel shows the recorded annual production (blue line) and the smoothed average behaviour (purple line) in Paraguay. The bottom panel reports the derived deviations (σ) as standardised anomalies (z).

### 3.1.2    Exposure of countries to drought

The impact of drought events on hydropower production in a given country is directly related to the occurrence of drought events in the water basins where major hydropower plants are located. To identify these basins, a Boolean mask is derived for each country using the global power plant database[4]. The mask highlights the basins where most of the power plants are located and excludes basins with small, isolated power plants. Only the basins that include major power plants

---

[4] https://datasets.wri.org/dataset/globalpowerplantdatabase

which collectively generate 95% of the total average capacity of the country are included in the analysis.

The Boolean mask obtained from this analysis is shown in Figure 5 and is used as an exposure map for assessing drought risk conditions at the country scale. In this case, the exposure represents the area of the country that is exposed to a drought risk specifically for hydropower production. This approach allows for a more accurate assessment of the impact of drought events on hydropower production in each country. By identifying the specific basins where major hydropower plants are located, policymakers and energy planners can better understand the potential impact of drought events on the energy sector and take appropriate measures to mitigate the risks.

It is important to note that the impact of drought on hydropower production is not limited to the direct effect on water availability. Drought events can also lead to increased sedimentation in reservoirs, reduced water quality, and damage to infrastructure, all of which can affect the efficiency and reliability of hydropower plants. Therefore, a comprehensive assessment of the drought risk conditions in the basins where major hydropower plants are located is crucial for ensuring the resilience of the energy sector in the face of climate change and other environmental challenges.
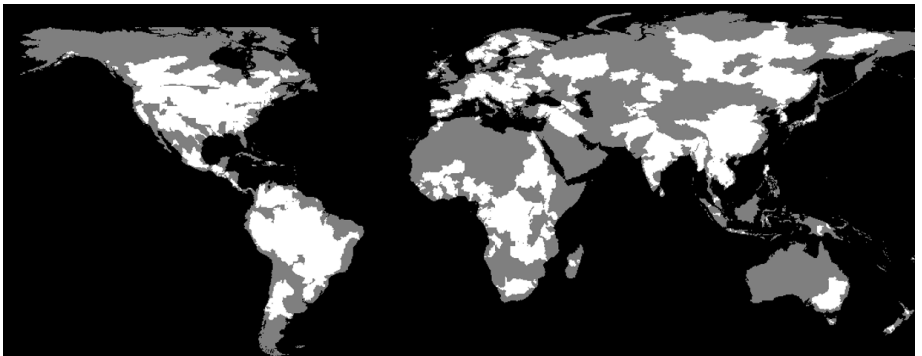
Figure 5. Boolean mask highlights (in white) the water basins where major hydropower plants are located for each country.

### 3.1.3    Assessment of the damage function

The study uses the monthly time series of the three drought indicators, namely SPI-6, SSI, and SMA (as described in section 3), to assess the fraction of the exposed area under drought conditions. The threshold value of -1 is used for each monthly data and for each indicator to determine the area under drought, as shown in Figure 6 for SPI-6. It is important to remember that the area under drought in a country is computed only in the portion of the territory covered by catchments where a considerable amount of hydropower is installed (at least 95% of the total hydropower production of a country). This allows avoiding correlations to droughts that occurred in areas that are not connected with hydropower production.
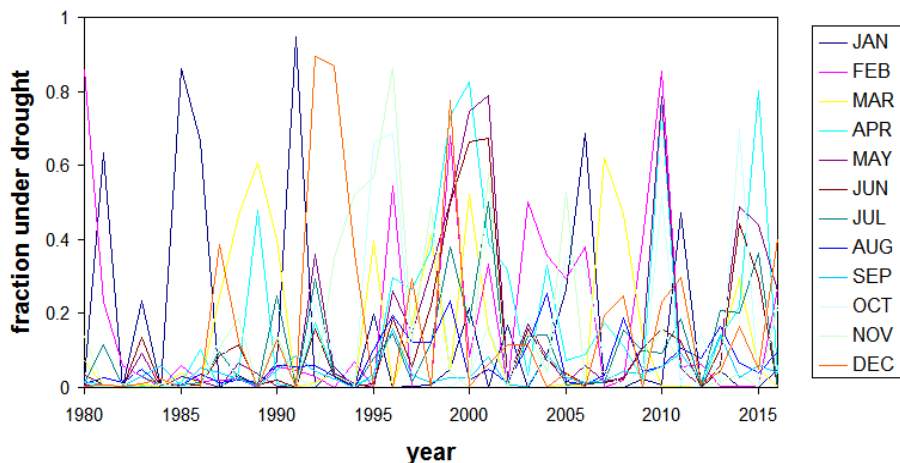


Figure 6. Example of the data extracted for each country starting from the time series of maps of drought indicators (SPI-6 in this example for Madagascar).

Once a time series is produced (36 years x 12 months) for each of the 20 countries and for each of the three considered indicators, a set of correlation analyses is performed between these time series and the drought impacts expressed in terms of deviations from the smoothed average hydropower production (z, see section 3.1.1). While the hydropower production time series has only one value per year, the drought indicators have monthly frequency. Hence, a correlation value (Pearson coefficient, r) is computed between each monthly time series (12 series) and z. In order to explore the possibility that in some rainfall regimes also data in the preceding year may be relevant, time series for the 4 antecedent months are also considered, for a total of 48 r values for each country (12+4 correlation analyses for each of the 3 indicators). The following scheme exemplifies the procedure adopted to compute the set of r values for a given indicator (X) and a given country:

$$r_{X1} = corr\{X_{m9y-1}, X_{m9y}, X_{m9y+1}, ..., X_{m9yn-1}\} \text{ vs. } \{z_y, z_{y+1}, z_{y+2}, ..., z_{yn}\}$$

$$r_{X2} = corr\{X_{m10y-1}, X_{m10y}, X_{m10y+1}, ..., X_{m10yn-1}\} \text{ vs. } \{z_y, z_{y+1}, z_{y+2}, ..., z_{yn}\}$$

$$r_{X3} = corr\{X_{m11y-1}, X_{m11y}, X_{m11y+1}, ..., X_{m11yn-1}\} \text{ vs. } \{z_y, z_{y+1}, z_{y+2}, ..., z_{yn}\}$$

$$r_{X4} = corr\{X_{m12y-1}, X_{m12y}, X_{m12y+1}, ..., X_{m12yn-1}\} \text{ vs. } \{z_y, z_{y+1}, z_{y+2}, ..., z_{yn}\}$$

$$r_{X5} = corr\{X_{m1y}, X_{m1y+1}, X_{m1y+2}, ..., X_{m1yn}\} \text{ vs. } \{z_y, z_{y+1}, z_{y+2}, ..., z_{yn}\}$$

$$...$$

$$r_{X16} = corr\{X_{m12y}, X_{m12y+1}, X_{m12y+2}, ..., X_{m12yn}\} \text{ vs. } \{z_y, z_{y+1}, z_{y+2}, ..., z_{yn}\}$$

where $m$ and $y$ represent the month and the year, respectively, and $n$ is the total number of available years.

The goal of this cross-correlation analysis is to detect multi-month consecutive periods where each indicator can be considered a good proxy of the impacts. Negative correlations are expected and they indicate that production is reduced when the area under drought is high. While there is a clear context of manifestation for these correlation patterns between production and the

selected indexes, this link can manifest in complex manners depending on climate, catchments' morphology as well as reservoir management, therefore an optimal combination of indicators needs to be selected for every country considered.

An example of a set of cross-correlation analyses is reported in Figure 7 for SPI-6 data over NZL.
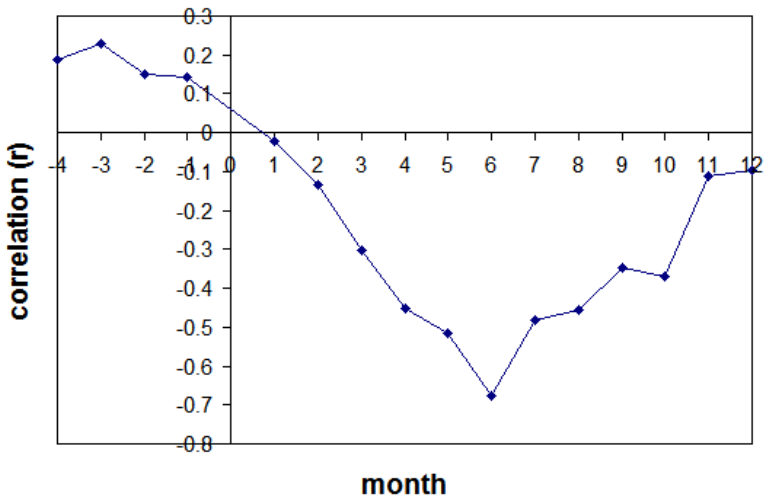


Figure 7. Example of the set of cross-correlation analysis for SPI-6 for a given country (NZL).

To identify the optimal period to capture the dynamic of drought impacts, a two-step procedure was implemented. The first step allows the identification of the period of consecutive months with the highest correlation with the reduction in hydropower production. The average correlation for all the consecutive periods of length between 3 (minimum length of a drought, as defined in section 3) and 8 months (half of the total length) is computed (for a total of 69 combinations). Among this set of periods, we selected the period that maximises the combination of the average correlation and maximum length as the optimal period to capture the dynamic of drought impacts. This was done by selecting among the cases in the 5-th percentile in terms of

average correlation (negative values) the one with the longest duration. For the previous example in Figure 7, the 5 months period between months 4 and 8 is detected as optimal for SPI-6.

It is worth remarking that the same procedure is applied to all three indicators independently, hence a set of 3-8 monthly series is selected for each index to be used for the successive multi-regression analysis.

The second step of the procedure aims at filtering only the statistically significant months in the identified periods. The monthly time series within the optimal periods for each index are pooled together for a multi-regression analysis to reproduce the temporal variability of hydropower production. In order to remove redundant information and contributions to the regression that are not statistically significant, the p-value associated to each multi-regression parameter is used to remove any non-significant contribution. In the specific example in Figure 7, the month at peak correlation (month 6) is the only one that significantly contributes to explaining the observed overall variability of hydropower production (with the other months bringing redundant information), hence the only month included in the multi-regression analysis for SPI-6. For the other two indicators (for the New Zealand case), the data for months 7 and 8 (SSI) and 6 (SMA) are the ones included, for a final multi-regression analysis based on 4 time series (SPI-6 for month 6, SSI for months 7 and 8, SMA for Month 6). Examples of this analysis are reported in Figure 8 for Madagascar (MDG, left panel) and New Zealand (NZL, right panel). The error bars in the figure are derived from the confidence interval computed considering both residual standard error and the variability of the predictor variables.
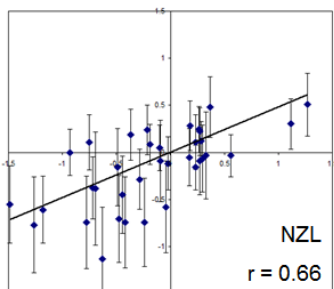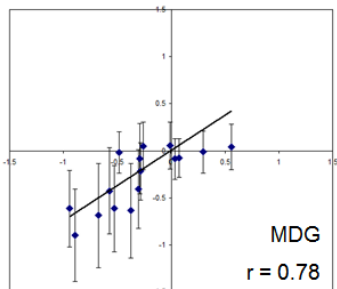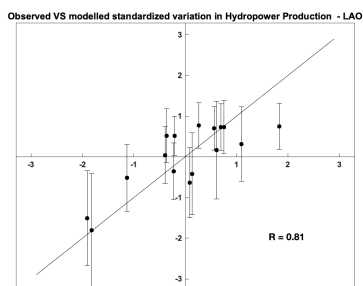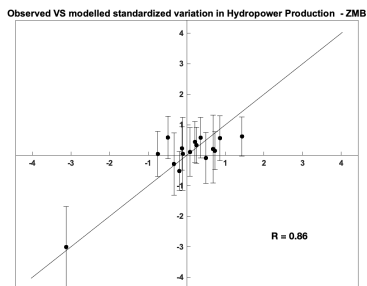
Figure 8. Correlation between observed (x-axis) and modelled (y-axis) standardised variations (z) in hydropower energy production for the test cases of Madagascar (MDG, left panel) and New Zealand (NZL, right panel).

Although there is a clear physical causal relationship between the three selected indexes and water availability in the considered catchments for hydropower production, actual fluctuations/reductions in production records do not depend only on the climatic variability (despite the effort in removing some of the long-term effects, as described in section 3.1.1). This accounts for the portion of the variance remains unexplained by the drought indicators.

Figure 9 shows some additional graphics showing the correlation between the observed and simulated for the countries considered in the final Hydropower loss analysis.
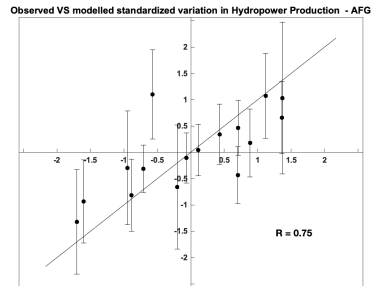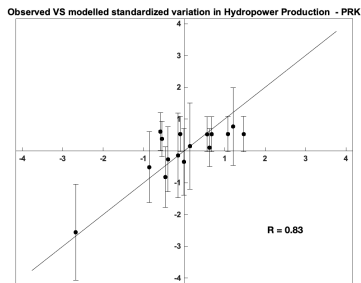
Figure 9. Correlation between observed (x-axis) and modelled (y-axis) standardised variations (z) in hydropower energy production for some of the analysed countries.

The results of the multi-regression analysis are summarised in Table 2, reporting the obtained multi-regression $R^2$ and the corresponding statistical significance (p-value). The value of σ is also reported for each country, representing the reduction in hydropower production (P) with an expected return period of between 6 and 7 years in the present climate (frequency, $f_{present}$, of about 0.16 considering a standard Gaussian distribution).

Table 2 Summary of the main outcomes and performance of the multi-regression analysis.

| ISO | Country name | Avg. Fluctuation in hydro production (σ) (TWh) | $R^2$ | p-value |
|---|---|---|---|---|
| AFG | Afghanistan | 0.1 | 0.56 | 0.02 |
| ALB | Albania | 1.2 | 0.35 | 0.01 |
| BTN | Bhutan | 1.1 | 0.58 | 0.08 |
| COD | Congo (Dem. Rep.) | 1.1 | 0.61 | 0.06 |
| CRI | Costa Rica | 0.6 | 0.59 | 0.00 |
| ETH | Ethiopia | 1.4 | 0.46 | 0.05 |
| GEO | Georgia | 0.8 | 0.38 | 0.11 |
| KGZ | Kyrgyzstan | 2.2 | 0.41 | 0.03 |
| LAO | Lao (People's Dem. Rep.) | 2.2 | 0.66 | 0.01 |
| LSO | Lesotho | 0.1 | 0.53 | 0.06 |
| MOZ | Mozambique | 2.0 | 0.37 | 0.12 |
| MWI | Malawi | 0.2 | 0.46 | 0.05 |

| NAM | Namibia | 0.2 | 0.45 | 0.06 |
|-----|---------|-----|------|------|
| NOR | Norway | 7.6 | 0.50 | 0.00 |
| NPL | Nepal | 0.3 | 0.57 | 0.01 |
| PRK | Korea (Dem. People's Rep.) | 1.7 | 0.68 | 0.02 |
| PRY | Paraguay | 6.7 | 0.46 | 0.05 |
| TJK | Tajikistan | 1.3 | 0.43 | 0.07 |
| UGA | Uganda | 0.5 | 0.42 | 0.08 |
| ZMB | Zambia | 1.8 | 0.75 | 0.01 |

The outcomes of the multi-regression analysis show some variability in the obtained coefficients of determination ($R^2$), which quantifies the extent to which the model accurately reproduces observed results by measuring the proportion of the total variation in the results that can be attributed to the model. Coefficients of determination ranges between $0.51 \pm 0.11$, with the highest values observed for Korea (Dem. People's Rep.) and Zambia, and the lowest values for Albania, Georgia and Mozambique. For few countries, a p-value $> 0.05$ indicates a not satisfactory reproduction of the hydropower production with the adopted approach, reducing the capacity of the analysis to accurately attribute reductions in hydropower production to droughts. It is possible that in such cases the z values used as a proxy variable of impacts of drought are in fact related to other issues, thus they cannot be fully explained by drought indices.

In order to assess the frequency of extreme hydropower production reductions in the future scenarios, the study applies the multi-regression functions, calibrated on the observed data in the present climate, to the two future scenarios, and computes the frequency of a reduction of more

than σ in the production low emission scenario SSP1-2.6 and high emission scenario SSP5-8.5, indicated as $f_{low}$ and $f_{high}$, respectively. Values of $f_{low}$ or $f_{high}$ higher (lower) than $f_{present}$ represent an increase (decrease) in the occurrence of significant reductions in the production (P) attributable to drought shocks.

The maps in Figure 10 show the spatial distribution of these results. These numbers represent the increase (decrease) in the frequency of significant reduction in hydropower losses compared to the present. For example, a value of 2 in red shades means that in the future scenario, the frequency of such extreme reductions is projected to increase twofold compared to the present.

changes in the frequency of low hydropower production (P < μ-σ) for the low scenario

changes in the frequency of low hydropower production (P < μ-σ) for the high scenario
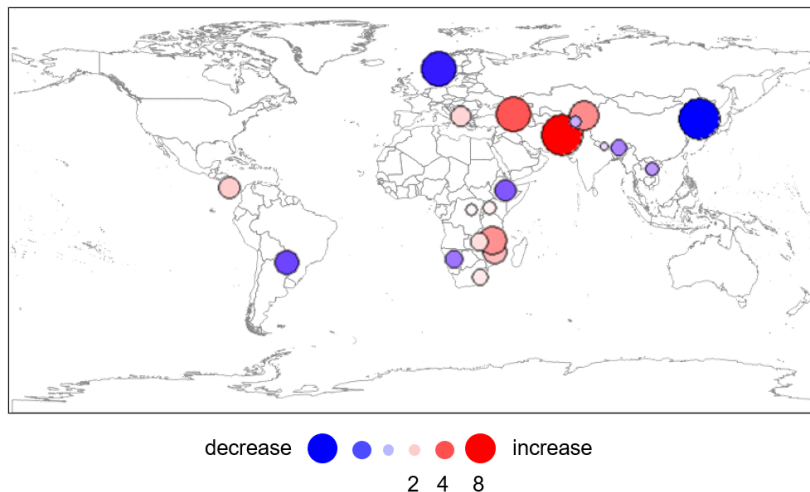


decrease ●  ● ● ● ●  increase

2  4  8

Figure 10. Spatial distribution of the increase (in red shades) or decrease (in blue shades) in the frequency of extreme reductions compared to the present. The upper panel reports the results for the low emissions scenario (SSP1-2.6), whereas the lower panel reports the same for the high emissions scenario (SSP5-8.5).

Notably, the frequency of extreme reductions in hydropower production is projected to increase over the Middle East and Eastern Africa, whereas a decrease in the frequency of extreme low production is projected over Norway, Eastern Asia and south-eastern South America. These results have important implications for energy planning and policy-making, as they highlight the need to develop strategies to enhance the resilience of the energy sector in regions where the frequency of extreme reductions in hydropower production is projected to increase. The study provides valuable insights for policymakers and energy planners to develop adaptation measures and strategies to mitigate the impacts of climate change on the energy sector.

The plot in Figure 11 shows the relationship between $f_{low}$ and $f_{high}$ (both normalised as a ratio of $f_{present}$). This plot highlights how the frequency of events characterised by extreme reductions in

hydropower production is on average 29% higher for the high scenario compared to the low scenario over the 20 countries analysed. This information is useful to understand the impact that mitigation strategies (i.e. keeping emissions close to the 2.6 scenario rather than 8.5) may have in hydropower production.
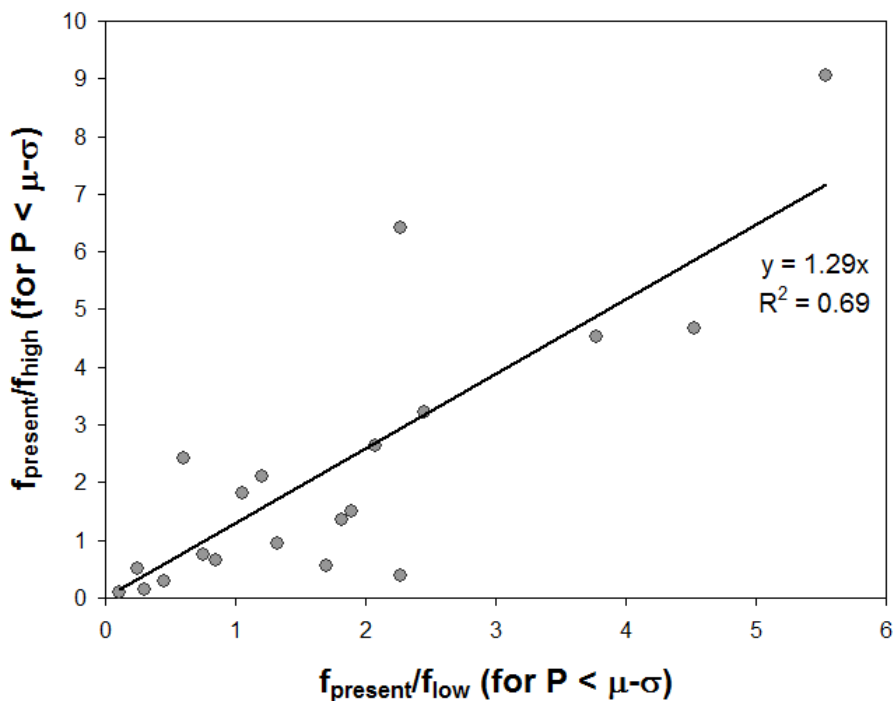


Figure 11. Relation between the frequency of extreme reductions in hydropower production ($P < \mu-\sigma$) in the low ($f_{low}$) and high ($f_{high}$) emission scenarios, expressed as a ratio with the present frequency ($f_{present}$).

The final part of the study conducts a drought risk assessment in terms of losses to the hydropower production sector, expressed in TWh, by considering the yearly average inter-annual fluctuation in hydropower production (as reported in Table 2) and the outcomes of the multi-

regression analysis including its uncertainty (i.e., the confidence interval). Including uncertainty in the estimation of risk metrics is crucial in this context, as it can be significant in some countries and is a fundamental characteristic of the probabilistic approach.

To account for uncertainty, the analysis employs a Monte Carlo simulation using the modelled standardised inter-annual variability in hydropower production (σ) and its uncertainty (confidence interval in the multi-regression parameters) as inputs of a Gaussian probability distribution.

In particular, the 'predict' function in R allows the estimation of confidence intervals for the predicted response or mean at specific values of the predictor variables in linear regression models. The confidence intervals are derived using the standard error of prediction, which considers the residual standard error and the variability of the predictor variables. By fitting a Gaussian distribution around the mean values obtained from linear regression using confidence intervals, we can derive Monte Carlo simulations that capture the parameter uncertainty. The width of the distribution is determined by the width of the confidence intervals.

Using the fitted Gaussian distribution, we generate random samples that represent different possible outcomes within the confidence intervals. These samples allow us to simulate a range of potential responses, accounting for the uncertainty in the linear regression model.

A sample of possible 1000 years of possible realisations is generated for each year. The analysis is performed under current climate conditions and projected climate conditions (low - SSP1-2.6 and high - SSP5-8.5 emission scenarios).

The simulated series standardised values are then converted into units of hydropower production (in TWh) using the conversion factors listed in Table 2. Risk metrics in terms of Annual Average Loss and Probable Maximum Loss for assigned return periods are computed by considering only the years with loss in hydropower production.

Table 3 reports the Annual Average Loss in TWh/year for the current climate and for low and high-emission scenarios for the 20 countries considered. The results confirm the trend shown in the changes of frequency of significant drop in production, with some countries, such as Costa Rica, projected to face a substantial increase in losses with a 300% increase in the low-emission scenario and a 500% increase in the high emission scenario. On the other hand, other countries, like South Korea, are projected to experience a significant decrease in hydropower production losses. In the present climate we observe that less than 50% of the countries experience an average loss of hydropower production that exceeds 5% of their total production, with a peak for Lesotho that exceeds 12% of the total production. However, when the low-emission scenario is considered the number of countries experiencing losses greater than 5% in production rises to more than 60%, with peaks in Lesotho and Costa Rica that largely exceed 15% of the total production. In the high-emission scenario, this percentage rises to 65% with 7 countries experiencing losses greater than 10% in production, and Lesotho, Costa Rica and Afghanistan experiencing losses of about 30% with respect to their total production. This last scenario would be hard to cope with by these national economies.
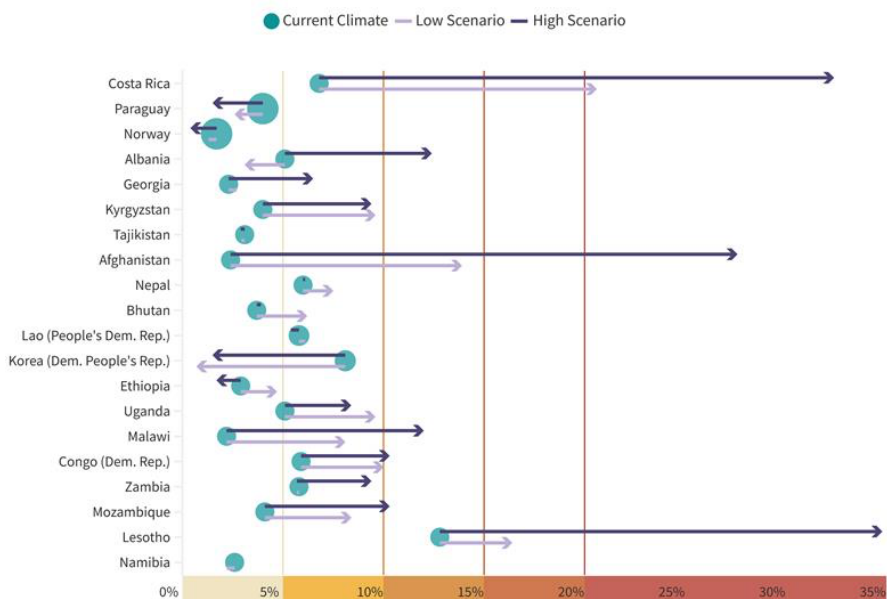
Table 3 Absolute and relative Annual Average Loss (AAL) to hydropower production [TWh/y] in current, low and high emission scenarios. Brown shading represents the severity of the AAL/(average production ratio) (classes: <5%, 5%-10%, 10%-15%, 15%-20%, >20%)

| ISO | Country name | AAL in hydropower production | | | AAL/(average annual hydro-production) | | |
|---|---|---|---|---|---|---|---|
| | | Current Climate [TWh/y] | Low Scenario SSP1-2.6 [TWh/y] | High Scenario SSP5-8.5 [TWh/y] | Current Climate [%] | Low Scenario SSP1-2.6 [%] | Scenario SSP5-8.5 [%] |
| LSO | Lesotho | 0.07 | 0.08 | 0.16 | 12.9% | 15.6% | 31.5% |
| PRK | Korea (Dem. People's Rep.) | 1.01 | 0.09 | 0.19 | 8.1% | 0.7% | 1.5% |
| CRI | Costa Rica | 0.52 | 1.57 | 2.47 | 6.8% | 20.6% | 32.3% |
| NPL | Nepal | 0.23 | 0.29 | 0.23 | 6.0% | 7.5% | 6.1% |
| COD | Congo (Dem. Rep.) | 0.52 | 0.88 | 0.79 | 5.9% | 10.0% | 9.0% |
| LAO | Lao (People's Dem. Rep.) | 0.98 | 1.03 | 0.91 | 5.8% | 6.1% | 5.4% |

| ZMB | Zambia | 0.74 | 0.73 | 1.21 | 5.8% | 5.7% | 9.5% |
|-----|--------|------|------|------|------|------|------|
| ALB | Albania | 0.29 | 0.18 | 0.71 | 5.1% | 3.1% | 12.3% |
| UGA | Uganda | 0.15 | 0.28 | 0.25 | 5.1% | 9.6% | 8.5% |
| MOZ | Mozambique | 2.29 | 1.47 | 0.86 | 4.1% | 2.6% | 1.5% |
| KGZ | Kyrgyzstan | 0.54 | 1.29 | 1.26 | 4.0% | 9.7% | 9.5% |
| PRY | Paraguay | 0.61 | 1.26 | 1.55 | 4.0% | 8.4% | 10.3% |
| BTN | Bhutan | 0.28 | 0.48 | 0.30 | 3.6% | 6.3% | 4.0% |
| TJK | Tajikistan | 0.52 | 0.52 | 0.49 | 3.0% | 3.0% | 2.9% |
| ETH | Ethiopia | 0.31 | 0.49 | 0.18 | 2.9% | 4.7% | 1.7% |
| NAM | Namibia | 0.03 | 0.03 | 0.03 | 2.6% | 2.2% | 2.6% |
| AFG | Afghanistan | 0.02 | 0.12 | 0.24 | 2.4% | 13.9% | 27.5% |
| GEO | Georgia | 0.20 | 0.23 | 0.55 | 2.3% | 2.7% | 6.5% |

| MWI | Malawi | 0.04 | 0.14 | 0.21 | 2.2% | 8.1% | 12.0% |
| NOR | Norway | 2.29 | 1.71 | 0.54 | 1.7% | 1.3% | 0.4% |



Figure 12 Annual Average Loss (AAL) to hydropower production [TWh/y] in current, low and high emission scenarios. Red shading represents the severity of the AAL/(average production ratio) (classes: <5%, 5%-10%, 10%-15%, 15%-20%, >20%)

Figure 12 graphically represents the information content of Table 3.

These findings have important implications for energy planning and policy-making, as they highlight the need to develop strategies to enhance the resilience of the energy sector in regions where losses in hydropower production are projected to increase. Overall, this approach allows for a comprehensive assessment of the impact of drought events on hydropower production in countries that heavily rely on hydropower, taking into account the specific basins where major hydropower plants are located and the dynamic of drought impacts.

Figure 13 displays an example of Probable Maximum Loss (PML) curves for countries in Europe, East Asia, central and South America. While trends in Annual Average Loss (AAL) are more consistently pointing towards an exacerbation of losses in projected climates, in terms of PML the behaviour in respect to climate change impacts shows a greater variability. It is worth analysing the behaviour of North Korea where the high emission scenario (SSP5 8.5) has a higher AAL than the low scenario (SSP1 2.6) but the PML curve for the high return period shows the opposite trend. This peculiar situation can be explained by changes in the frequency of less severe droughts, which are projected to increase in the high scenario, and a simultaneous decrease in the frequency of more severe droughts. The former dominates the AAL estimate, while the latter dominates the PML curve.
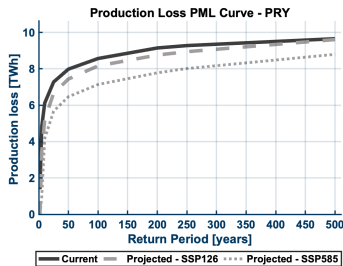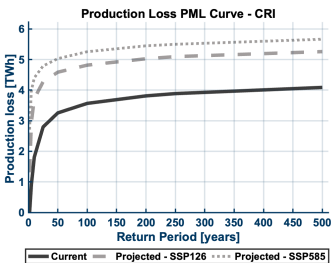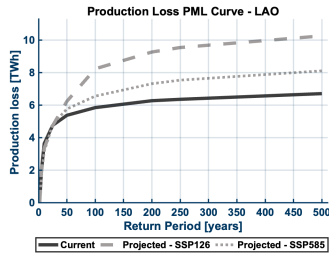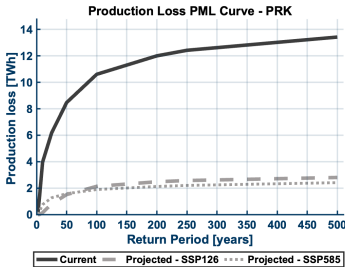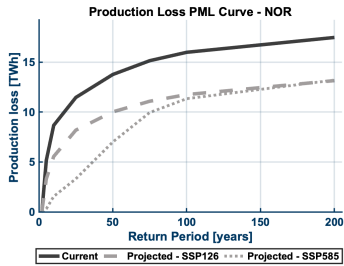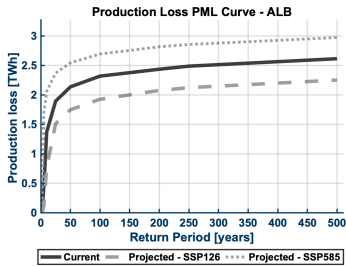
Figure 13. PML curves for hydropower production loss [Twh] in current and low and high emission scenarios for the countries selected in Europe, East Asia, central and South America.
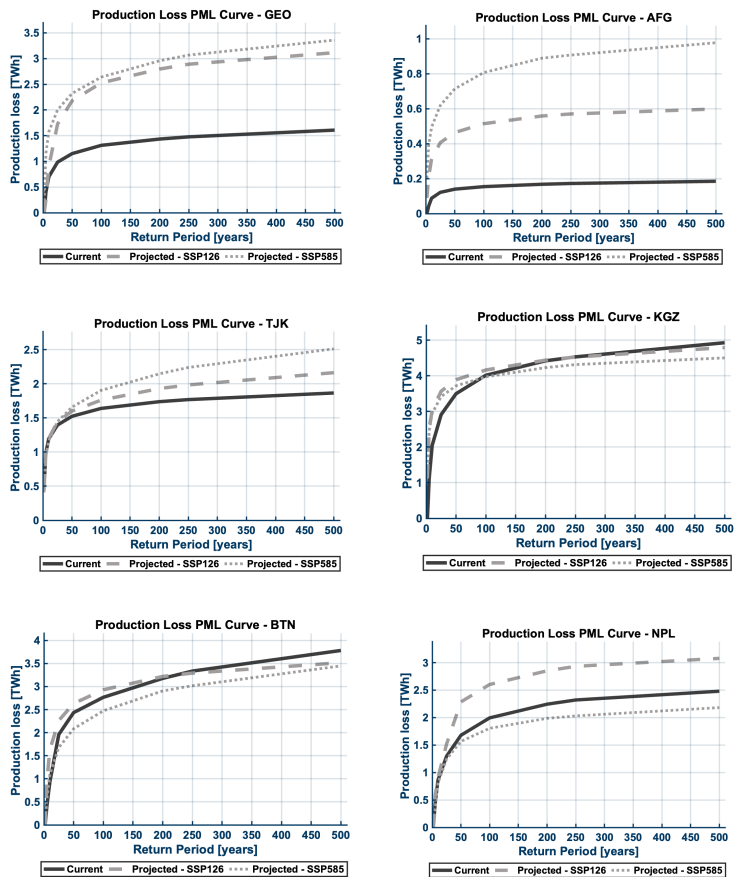
Figure 14. PML curves for hydropower production loss [Twh] in current and low and high emission scenarios for the countries selected Eastern Europe and Central Asia.

Figure 14 shows similar information for the Balkan area and Central Asia where trends of climate change are more consistently pointing towards more severe conditions for hydropower

production for high return period events. Figure 15 analyses the countries in East and Central Africa. East Africa shows higher losses for both projected climates while Central Africa shows an evident worsening of the conditions only when SSP5 RCP8.5 is considered. Similar consideration can be done for the southern African region moving from East to West (Figure 16).
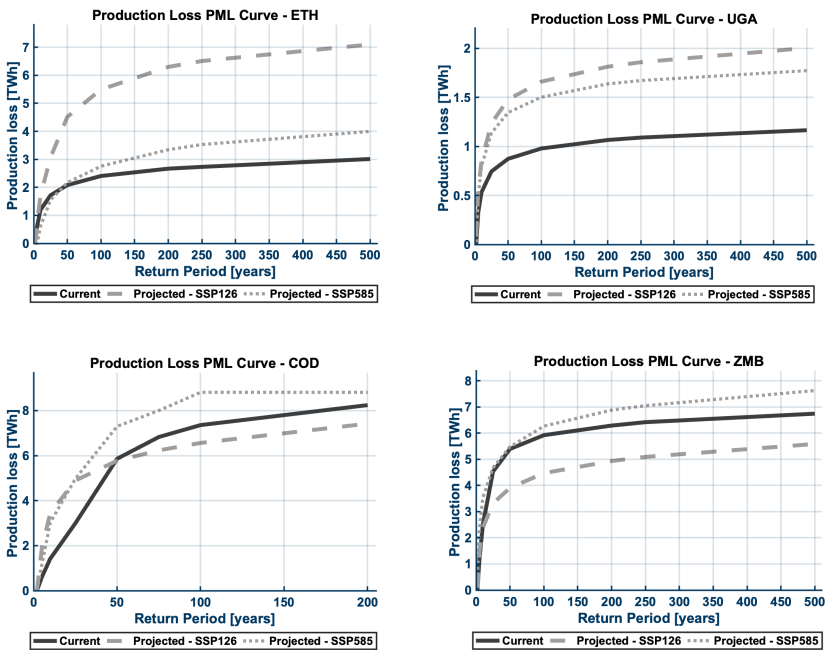


Figure 15. PML curves for hydropower production loss [Twh] in current and low and high emission scenarios for the countries selected in Central and East Africa.
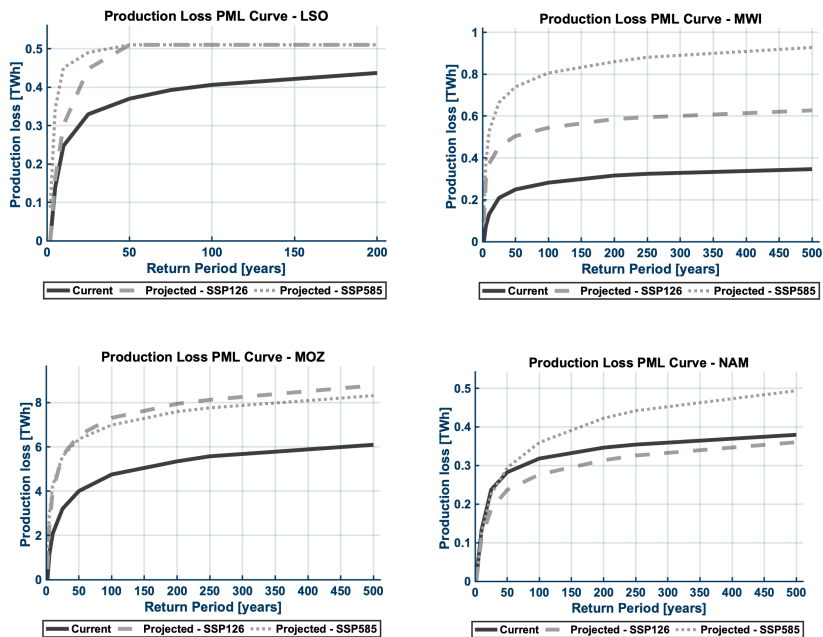
Figure 16. PML curves for hydropower production loss [Twh] in current and low and high emission scenarios for Southern Africa.

## 1.1 Drought impacts on total water availability

Water availability can deeply influence the socio-economic development of countries and its limitations represent a threat to livelihood in increasing parts of the world. The impact of water availability is commonly studied in relation to water demand or water use to identify water stress conditions. Many parts of the world are struggling with water scarcity conditions, which generally refers to a prolonged condition wherein demand for water by all sectors, including the environment, cannot be satisfied fully due to the impact of water use on supply or quality of water [Falkenmark et al., 1989; Alcamo et al., 2000; Vörösmarty et al., 2000].

There are several studies that analyse the water stress conditions for a country or region and they refer to different indexes able to capture the imbalances between water demand or use and water availability (Wang et al., 2021). One of the widely used approaches to quantify water availability is based on the demand-to-supply ratio (Hoekstra et al., 2012). In recent years, these approaches have been modified to account for the need to preserve the ecosystem and the possibility of reusing water resources in more sustainable systems (Pastor et al., 2014).

Among the different possibilities in this study, we opted for the Water Use-To-Availability Ratio index also known as the water criticality index (Alcamo et al., 2000).

$$Water\ Criticality\ Index\ (WCI) = \frac{Total\ Water\ Withdrawal}{Water\ Supply} \quad (1)$$

The choice was guided by the fact that there are recognized and accepted thresholds in literature and among practitioners to address water stress based on the WCI. Most water scarcity studies, categorize a region or a country into severe water scarcity (>40%), water scarcity (20–40%), moderate water scarcity (10–20%) and low water scarcity (<10%). The Water Resources Institute Water Risk Atlas[5] expands this categorization with two additional classes: between 40% and 80% and above 80%. These threshold values have been adopted by the United Nations (Raskin et al., 1997) and the European Environment Agency (EEA, 2009).

Spatial and temporal scale of the assessment depends on data availability. Given that data on water consumption/demand are usually not available at detailed spatial and temporal scales, long-term (e.g., 30-year) average values at country scales are used. In contrast, water supply information can be more easily inferred from the outcomes of hydrological models. The study is conducted on a yearly temporal scale to account for significant inter-annual variations in water availability and investigate frequency and intensity of annual water stress conditions. The

---

[5] https://wri.org/aqueduct

temporal dimension allows unveiling situations where a country, although not classified in water scarcity condition over a long period, can still experience severe water stress in some years.

In order to evaluate the numerator of equation (1) we referred to the data available in AQUASTAT[6] and more specifically to the total water withdrawal that includes water withdrawal for different uses: domestic and industrial use, agriculture, and livestock. The total water withdrawal estimate in Aquastat is derived through a combination of data collection and estimation methods. Acquastat gathers information from various sources, including national statistical agencies, government reports, research institutions, and other relevant organizations. In cases where comprehensive data is lacking or incomplete, Aquastat may employ estimation and extrapolation methods to derive total water withdrawal estimates. This involves using available data from specific regions or sectors and extrapolating it to estimate water use for the entire country. It is important to note that the accuracy and reliability of the total water withdrawal estimates in Aquastat can vary depending on the availability and quality of data reported by countries. However, Aquastat represents the most authoritative source at global scale in this respect.

Aquastat provides an estimate of the present water withdrawal while we would need to project this water demand in future to assess water stress in projected climate conditions. The future variations in water withdrawal for a specific country can be influenced by several factors. The main driving factor is obviously population growth. If the population of a country continues to grow, the demand for water for domestic, industrial, and agricultural purposes will increase, potentially leading to higher water withdrawal rates.

Other driving factors are linked to economic growth and development that often result in increased water demand. As countries progress economically, industrial activities, manufacturing,

---

[6] www.fao.org/aquastat

and energy production tend to expand, leading to higher water withdrawal rates (Hernadez et al., 2020). Additionally, rising standards of living and changing consumption patterns can impact domestic water use. This is finally linked to the urbanization level.

Other factors can also influence the future values of water withdrawal such as changes in water management strategies, technological advancements, shifts in agricultural practices or changes in policy and governance. These last ones are however difficult to anticipate and model.

A multivariate regression analysis was performed including population and economic growth as well as urbanization. While the analysis shows a clear link to population growth, considering GDP and urbanization level does not add any significant contribution to the regression. Urbanization shows a correlation with domestic water withdrawal, but when the total water withdrawal is considered, this correlation becomes statistically non-significant. Therefore, projection of total water withdrawal has been linked to population growth alone to maintain the simplicity of the model. The United Nations projections of population for the end of the century (2080 as a reference year) have been used in this study to project the total water withdrawal at country level.

The denominator of Eq. (1) has been modeled using the outcomes of the hydrologic model continuum, similarly to the approach taken for the energy sector analysis. While some of the water stress and scarcity assessments are conducted on a grid scale, country, basin or sub-basin scales are considered more policy-relevant (Liu at al, 2017).

Specifically, in this study the water available for all sectors in each country is calculated by treating the whole country as a control volume and applying the following water balance equation at an annual scale:

$$\Delta S = Pr - ET + Q_{in} - Q_{out} \qquad (2)$$

Where P represent the cumulated value of Precipitation entering the control volume, ET the evapotranspiration going out of the control volume, while Qin and Qout are respectively the discharge entering and exiting the control volume both from surface and sub surface fluxes. The concept is illustrated in Figure 13.
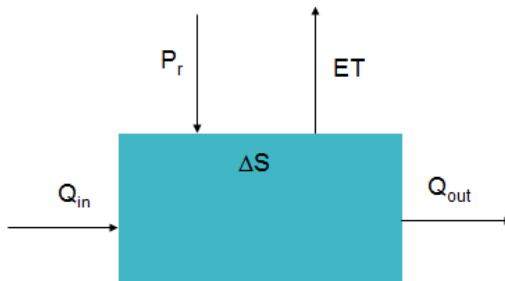


Figure 13 Computation of the total water supply (see Eq. 1). starting from the outputs of the Continuum model.

$\Delta S$ in equation (2) is used as a denominator in the WCI computation. It is important to note that a country cannot be considered a water-isolated body like a water basin. Therefore, the average inflow and outflow from neighbouring countries must be taken into account to accurately estimate the water availability for the different uses. The annual water balance has been performed for each catchment in the country and inflows and outflows on boundary cells (country borders) both for surface water and groundwater have been considered to close the annual balance and compute the available storage for exploitation. This includes the surface and groundwater exiting the country and flowing into other countries on in specific water bodies (lakes, seas, oceans). The water flowing out of the country can be considered in different ways. As an example, Aquastat considers the outflow to be fully exploitable by the country unless it is

subject to international water treaties that guarantee a certain annual amount of water resources to be transferred from one country to the other. In this study we decided to consider that a considerable part of the water flowing out of a country cannot be exploited for anthropic use for the following reasons.

A portion of the outflow at catchment level needs to be maintained to support ecosystems health. This proportion is normally considered between 20% to 30% of the natural flow. Another percentage remains unexploitable due to lack of infrastructure serving the different sectors. As a result of these considerations, two scenarios have been considered: One where only 40% of the total potential annual outflow can be exploited (low infrastructural water exploitation capacity) and one where 60% of the potential annual outflow is retained (high infrastructural water exploitation capacity).

We checked the robustness of this considerations as well as the ability of representing the actual water supply by computing the correlation between continuum water supply estimates and those of Aquastat considering a balance that best approximates the assumption within the acquastat quantifications. A correlation of 0.94 is found as represented in Figure 16.
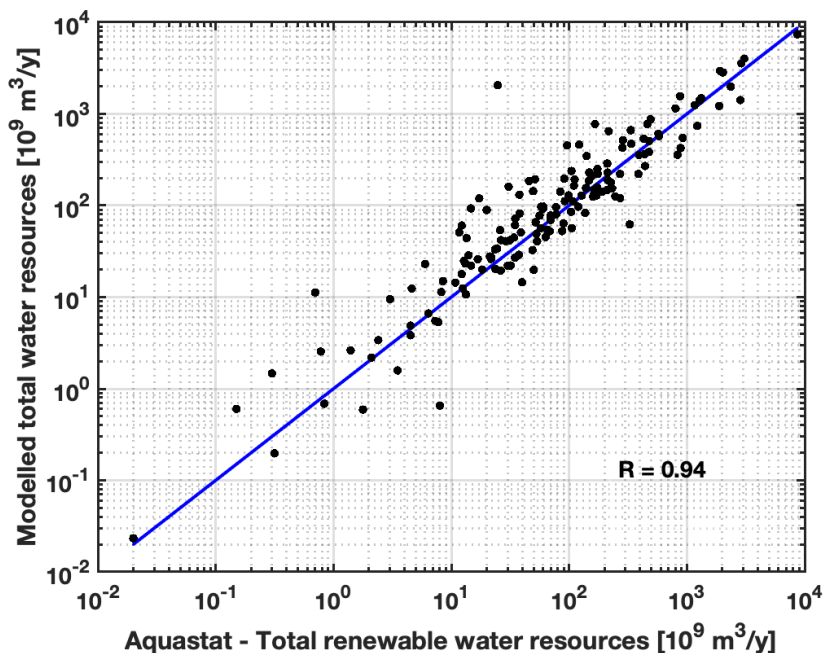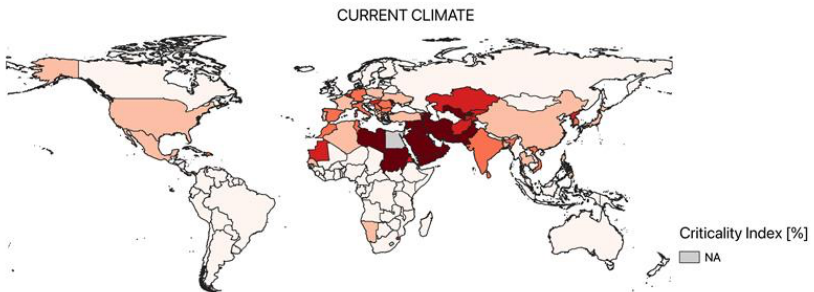
Figure 17 correlation between modelled total renewable water resources form the Continuum runs and the estimates of the same quantity in the Aquastat dataset.

Assessing water stress at the catchment level is crucial for understanding the spatial distribution of water resources and identifying areas where water scarcity may be a significant issue. However, obtaining accurate data on yearly water withdrawal disaggregated at the catchment level is a challenging task in a global study, this is especially true in large countries with complex water management systems. In addition, as part of multi-hazard risk assessment at global level, this study aims at providing risk quantification per country as performed for other hazards, to keep the same reference domain and facilitate the comparison across hazards, countries and climatic scenarios.

Despite this limitation, the approach used in this study provides a comprehensive understanding of the water resources available at the country level and put them in relation to the average water withdrawal.

For each modelled year, 37 years in the current climate and 50 years in both projected climate scenarios, the WCI was computed for each country using equation (1) quantifying the numerator and the denominator as explained previously in this section. As a result, 6 different time series per country were derived (3 in the high infrastructural capacity scenario and 3 in the low one). A Generalized Extreme Value distribution (GEV) was then fit to each of the obtained series and a Loss Exceedance Probability graph was generated for the 6 time-series in each country. By integration of these curves, an Annual Expected WCI value was derived in each condition for each of the countries. These Loss Exceedance Curves (LEC)represent the water stress induced by drought conditions created by the interannual variability of the water supply term. The curves offer a complete overview of the expected frequency of each water stress condition in the present and in the projected climate.



CURRENT CLIMATE

Criticality Index [%]
NA

In

SSP1-2.6



Criticality Index [%]

NA

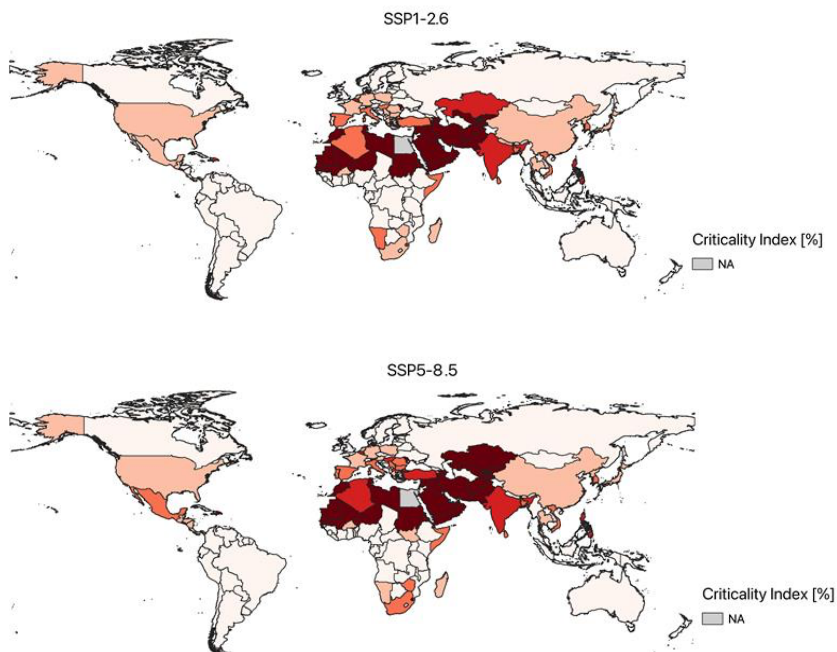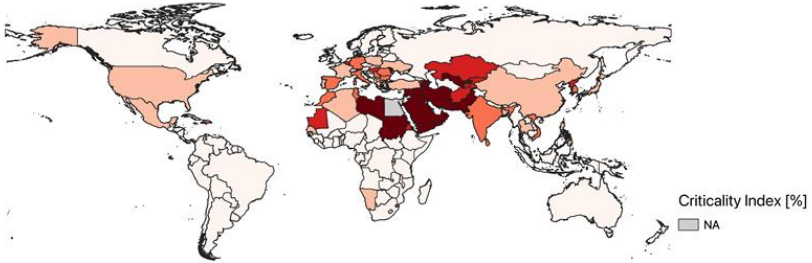SSP5-8.5



Criticality Index [%]

NA

Figure 18 (first panel) we plot the average annual Water stress conditions according to the usual definition of water stress using the WCI. Colours from light red to dark red depict water stress conditions from moderate water stress to extreme water stress. The Annual water stress condition can be considered as a long-term average and therefore linked to a persistent long-term condition in the country.

It is immediately visible how the Northern Africa region, the Arabic Peninsula, Caucasus as well as all the Western and Central Asia constitute a geographically continuous hotspot for water stress in the present climate. India is also experiencing challenging conditions due to the high

population values. However, in the case of india as well as in the case of some of the analysed countries their dimension is such that different climates are included and the water stress condition might be concentrated in specific portions of the territory, which aggravates condition that is already evident on a national scale.

Figure 18 mid and lower panels show the WCI for the low-emission and the high-emission future scenarios. in general, the pattern visible in the present climate is confirmed in both future scenarios. However, some areas seem to suffer a strong increase in the average water stress conditions. Western and Northern Africa are particularly affected in projected climate such as the Mediterranean Basin and Central America. Southern and Eastern Africa also experience an exacerbation of the water stress conditions in both scenarios.

CURRENT CLIMATE

Criticality Index [%]
NA

SSP1-2.6

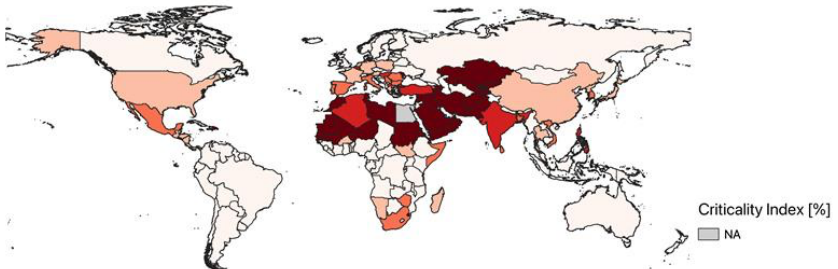Criticality Index [%]
NA

SSP5-8.5

Criticality Index [%]
NA
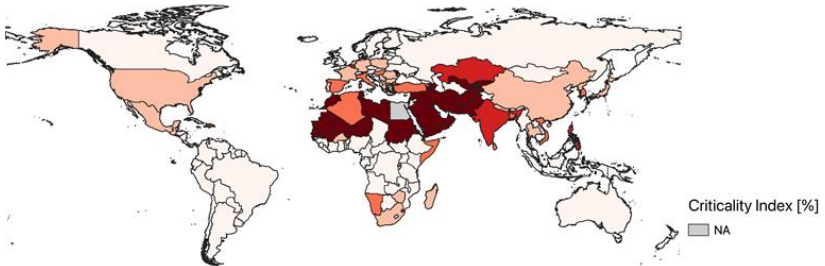
Figure 18 Annual Average Loss (in terms of WCI values) categorised for water stress levels. Darker colours express stronger water stress conditions. The first panel shows present climate conditions while the second and third panel present the low emissions and the high emission scenarios respectively.
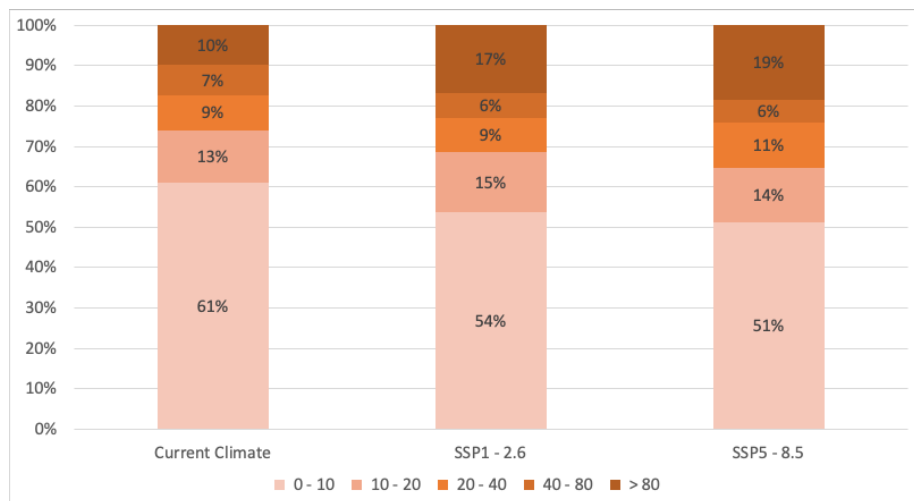


Figure 19 percentage of countries in the different water stress conditions for the three climates

Figure 19 shows the percentages of countries in the different classes of water stress. It is evident how climate change will globally worsen the water stress conditions increasing the percentage of countries in extreme water stress conditions from 10% to almost 20% when the high emission scenario is considered.

Figure 20 shows possible water stress for SSP5-RCP8.5 under the hypothesis of improving the Countries exploitation capacity (80% of the water flowing out of the countries is considered exploitable). Even if the general pattern does not change drastically, improvements can be noted in some countries such as India. While being far from giving the actual estimates this can be considered as a first indication of how impactful might be to strategically invest in the infrastructure to augment the countries capacity to exploit its water resources potential.
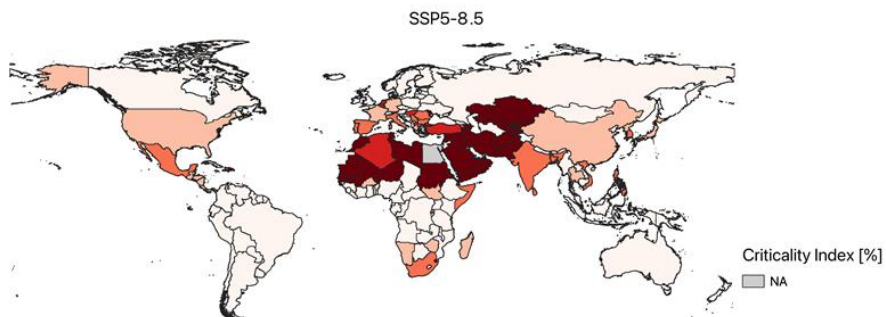
Figure 20 Annual Average Loss (in terms of WCI values) categorised for water stress levels. High emission scenario with improved infrastructure capacity for water exploitation (retention of up to 80% of the outflow surface water volume).

When LEC curves are considered new dimensions of the analysis can be discussed (Figure 21). The flatter the curve the more variable the impact of interannual variability of climate. This is especially evident among the curves presented in Zimbabwe where projected climate conditions not only will increase the average water stress but will also increase the difference in impacts among wetter and drier years. Opposite behaviour is shown in India where interannual variations are not particularly marked and it is the average condition that determines the water stress in the country. Zimbabwe and India change from moderate water stress to high water stress conditions in projected climate (both scenarios) calling for strategic thinking in the water sector for both countries. Similar comments can be done for Mexico that changes the water stress category in both future scenarios approaching critical conditions in the worst case (SSP5-RCP8.5). Spain, Cyprus and Lebanon are here presented to characterise the Mediterranean hotspot. While Lebanon is already experiencing a high water stress on average it is inclined in present climate to experience severe water stress conditions with an exceedance annual probability of 20% (once every 5 years). In future projections this probability increases up to 50% (once every 2 years) and 80% annual probability in the most extreme scenario. Even if with milder water stress conditions both Spain and Cyprus experience the same trend.
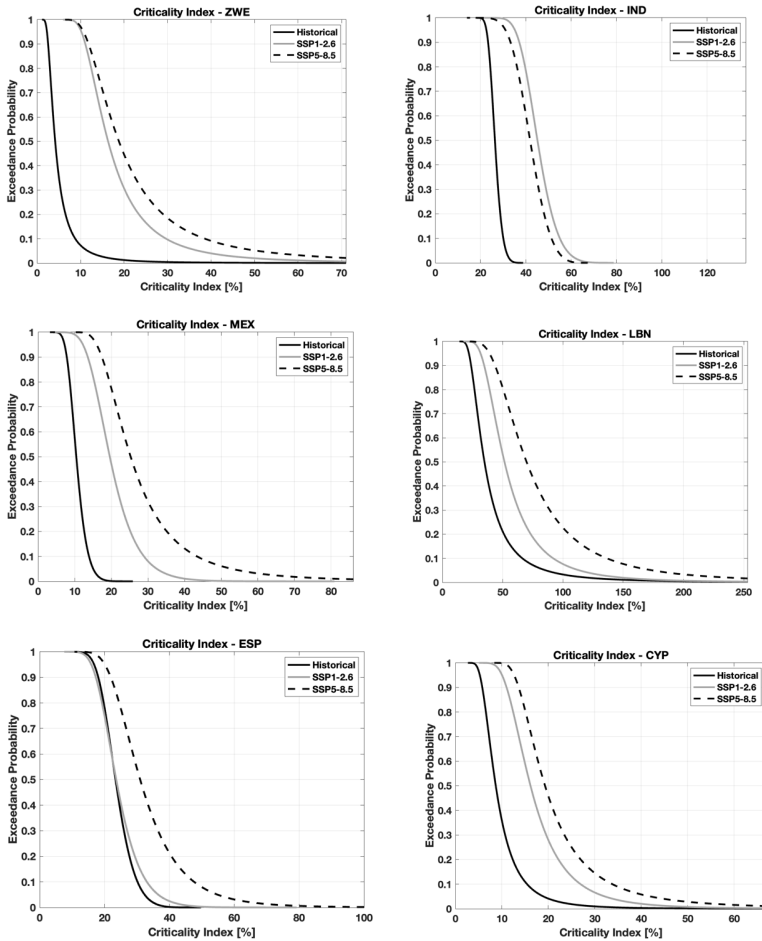
Figure 21 Loss Exceedance Curves for the WCI for sample countries worldwide.

In conclusion, climate change introduces uncertainties regarding future water availability. Assessing water stress conditions helps building resilience by identifying vulnerable areas and developing adaptive strategies. This allows governments to plan infrastructure investments strategically, ensuring a sustainable water supply for economic activities. By understanding the water needs of different sectors and considering climate change impacts, policymakers can support economic growth while avoiding disruptions due to lack of water. Possible interventions may include investing in water storage facilities, diversifying water sources, implementing efficient irrigation techniques, and promoting water-efficient technologies. By understanding the stress conditions, infrastructure investments can be tailored to address specific vulnerabilities and ensure long-term resilience.

## 1.2    Drought impacts on inland water transportation

Inland water transportation represents an environmental-friendly and often efficient mode of transport, and a key alternative to inland (e.g., roads and rails) transport in many regions of the world, including Asia-Pacific, Western Europe, Eastern Europe, North America, South America, Middle East, and Africa (Figure 22).
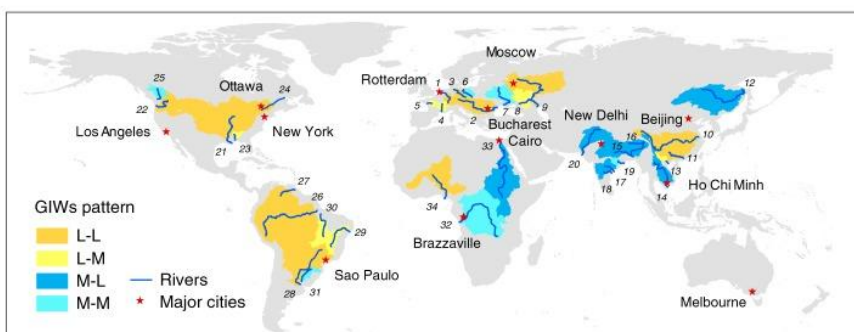


Figure 22 Map with the main inland waterways. Source: Wang et al., 2020

This mode of transport is affected by many natural and environmental conditions, mostly related to the control on water levels in the river network. In the context of drought, low flow conditions in free-flowing waterways (i.e., excluding regulated canals) may cause reduction in the cargo-carrying capacity, or even disruption in the service. Generally, the transport cost tends to increase with decreasing water levels, and large-size vessels are more cost-effective than small vessels.

Analyses of the impact of low flow conditions on waterway capacity often focus on critical (or bottleneck) sections, corresponding to the sections of the river where the fairway depth (i.e., average water level) is minimal. In addition, low flow conditions are generally more relevant during the low water season.

Since water levels are the most relevant quantities to manage waterways, a key step in the analysis of the effects of low flow on inland water transport is the conversion of flow volumes to water depth.

Following this overview, the proposed approach is structured as follow:

1) detect a river section representing the bottleneck condition;

2) define key water levels thresholds that are relevant for waterway management, as a function of the vessel types allowed in a specific waterway class;

3) convert water levels in flow conditions (thresholds);

4) compute the percentage of days when the flow falls below the defined threshold conditions.

Due to the difficulties to build a reliable connection between modelled flow conditions (from the CONTINUUM model) and water depth, this methodology is tested on a case study in the Rhine River basin in Europe.

The Rhine River is the major waterway in Europe, and it is classified as a class IVb waterway in the European classification (BMVI, 2014). This classification defines the characteristics of the vessels to be used to define the critical thresholds.

In the Rhine, the section in Kaub (Germany) is often identified as a critical section, as the shallowest part of the middle Rhine. The annual average flow at this section is about 2,000 $m^3$/s, with low flow regime during the period August-November. At the Kaub station, the low navigation water level (LNWL) is assumed to be 78 cm (water level at the gauge, not the river depth), corresponding to a flow condition that is exceeded in 345 days per year in the long term mean (Klein and Meissner, 2016). This value, corresponding to the 95-th percentile of the flow-duration curve, is modelled by CONTINUUM as a river flow of 1,000 $m^3$/s in the period 1979-2016.

In the bar plots in Figure 17 the percentage of days in which the flow is below the threshold value is reported for each year, representing the fraction of each year when the vessels cannot traverse at full capacity (related to the load fraction). Notable drought years, such as 2003 and 2011, can be observed in the graph.
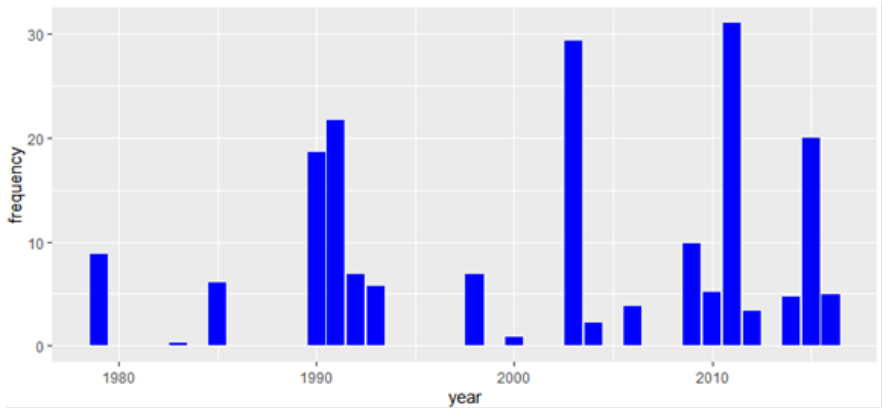


Figure 17 Percentage of days for each year with a flow below the threshold defining limitation in vessel loads.
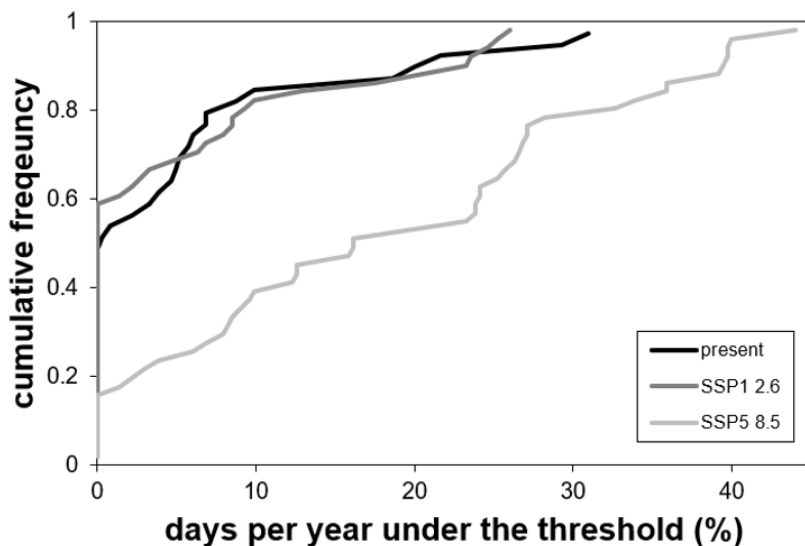
Figure 23 Cumulative empirical frequency curve of days under the navigation threshold (comparison among present climate and projected climate conditions).

The plot in Figure 23 reports the cumulative frequency distribution of these values (present), along with the analogous curves for the two future scenarios (RCP1 2.6 and RCP5 8.5). This plot shows how years with a small fraction of potential disruption are projected to be slightly lower than in the present for the scenario RCP1 2.6, whereas long interruptions are projected to become much more common in the RCP5 8.5. As an example, in both the present and for the scenario RCP1 2.6 almost 90% of the years are modelled to have less than 2 months of disruption (16% of days in a year) on average, but this frequency increases to almost 50% for RCP5 8.5. Obvious consequences for the inland water transportation can be derived from these results, including a reduced reliability of this transportation system in the most extreme scenario. Adopting this

simple methodology is a first approach on how drought impacts on inland water transportation for major waterways can be derived globally.

## 2    REFERENCES

Alcamo, J.; Henrichs, T.; Rösch, T. World Water in 2025-Global Modeling and Scenario Analysis for the World Commission on Water for the 21st Century; Kassel World Water Series; University of Kassel: Kassel, Germany, 2000.

BMVI,                    2014.                    Bundeswasserstraßenkarte                    DBWK1000. https://www.wsv.de/service/karten_geoinformationen/bundeseinheitlich/pdf/DBWK1000_Generaldirektion_2014.pdf

Cammalleri, C., Micali, F., Vogt, J. (2016). A novel soil moisture-based drought severity index (DSI) combining water deficit magnitude and frequency. Hydrol. Process. 30, 289-301.

EEA. Water Resources across Europe: Confronting Water Scarcity and Drought; European Environment Agency: Copenhagen, Denmark, 2009.

Hao, Z., Singh, V.P., 2015. Drought characterization from a multivariate perspective: A review. J. Hydrol. 527, 668-678. doi:10.1016/j.jhydrol.2015.05.031.

Hernandez, Y., Naumann, G., Corral, S. and Barbosa, P., 2020. Water footprint expands with gross domestic product. Sustainability, 12(20), p.8741.

Hoekstra A.Y., Mekonnen, M.M., Chapagain, A.K, Mathews, R.E., Richter, B.D., 2012. Global monthly water scarcity: Blue water footprints versus blue water availability PLoS One 7.

Klein, B., Meissner, D., 2016. IMPREX D9.1: Vulnerability of Inland Waterway Transport and Waterway Management on Hydro-meteorological Extremes.

Kummu M., Gerten, D., Heinke, J., Konzmann, M., Varis, O., 2014. Climate-driven interannual variability of water scarcity in food production potential: A global analysis Hydrol. Earth Syst. Sci. 18 447–61.

Liu, J.; Yang, H.; Gosling, S.N.; Kummu, M.; Flörke, M.; Pfister, S.; Hanasaki, N.; Wada, Y.; Zhang, X.; Zheng, C.; et al. Water Scarcity Assessments in the Past, Present, and Future. Earth's Futur. 2017, 5, 545–559.

Pastor, A.V., Ludwig, F., Biemans, H., Hoff, H., Kabat, P., 2014. Accounting for environmental flow requirements in global water assessments Hydrol. Earth Syst. Sci. 18 5041–59.

Raskin, P.; Gleick, P.; Kirshen, P.; Pontius, G.; Strzepek, K. Comprehensive Assessment of the Freshwater Resources of the World; Stockholm Environment Institute: Stockholm, Sweden, 1997.

Shukla, S. H., & Wood, A. W. (2008). Use of a standardized runoff index for characterizing hydrologic drought. Geophysical Research Letters, 35(2), 41–46.

Silvestro, F., Gabellani, S., Delogu, F., Rudari, R., and Boni, G., Exploiting remote sensing land surface temperature in distributed hydrological modelling: the example of the Continuum model, Hydrol. Earth Syst. Sci., 17, 39-62, doi:10.5194/hess-17-39-2013, 2013.

Silvestro, F., Gabellani, S., Rudari, R., Delogu, F., Laiolo, P., and Boni, G.: Uncertainty reduction and parameter estimation of a distributed hydrological model with ground and remote-sensing data, Hydrol. Earth Syst. Sci., 19, 1727-1751, doi:10.5194/hess-19-1727-2015, 2015. //www.hydrol-earth-syst-sci.net/19/1727/2015/hess-19-1727-2015.html

Wang, D., Hubacek, K., Shan, Y., & Liu, J. (2021). A Review of Water Stress and Water Footprint Accounting. Water, 13(2), 201. https://doi.org/10.3390/w13020201

World Meteorological Organization (WMO) and Global Water Partnership (GWP), 2016: Handbook of Drought Indicators and Indices (M. Svoboda and B.A. Fuchs). Integrated Drought Management Programme (IDMP), Integrated Drought Management Tools and Guidelines Series 2. Geneva

Yevjevich, V., 1967. An objective approach to definitions and investigations of continental hydrological droughts. Colorado State University, Fort Collins, Hydrology Paper 23.

Zelenhasić, E., Salvai, A., 1987. A method of streamflow drought analysis. Water Resour. Res., 23(1), 156-168.